

1 Disturbance of deep-sea environments induced by the M9.0 Tohoku Earthquake.

2

3 **Authors**

4 S Shinsuke Kawagucci<sup>1 2 \*</sup>, Yukari T. Yoshida<sup>3</sup>, Takuroh Noguchi<sup>4</sup>, Makio C. Honda<sup>5</sup>,  
5 Hiroshi Uchida<sup>5</sup>, Hidenori Ishibashi<sup>6</sup>, Fumiko Nakagawa<sup>6</sup>, Urumu Tsunogai<sup>6</sup>, Kei  
6 Okamura<sup>4</sup>, Yoshihiro Takaki<sup>3</sup>, Takuro Nunoura<sup>3</sup>, Junichi Miyazaki<sup>1 2 3</sup>, Miho Hirai<sup>3</sup>,  
7 Weiren Lin<sup>7</sup>, Hiroshi Kitazato<sup>3</sup>, and Ken Takai<sup>1 2 3</sup>.

8 **Affiliations**

9 1Precambrian Ecosystem Laboratory, Japan Agency for Marine-Earth Science and  
10 Technology (JAMSTEC), 2-15 Natsushima-cho, Yokosuka 237-0061, Japan.

11 2Submarine Resources Research Project, Japan Agency for Marine-Earth Science and  
12 Technology (JAMSTEC), 2-15 Natsushima-cho, Yokosuka 237-0061, Japan.

13 3Institute of Biogeosciences, Japan Agency for Marine-Earth Science and Technology  
14 (JAMSTEC), 2-15 Natsushima-cho, Yokosuka 237-0061, Japan.

15 4Center for Advanced Marine Core Research, Kochi University, B200 Monobe,  
16 Nankoku 783-8502, Japan.

17 5Research Institute for Global Change, Japan Agency for Marine-Earth Science and  
18 Technology (JAMSTEC), 2-15 Natsushima-cho, Yokosuka 237-0061, Japan.

19 6Faculty of Science, Hokkaido University, N10 W8, Kita-ku, Sapporo, 060-0810,  
20 Japan.

21 7Kochi Institute for Core Sample Research, Japan Agency for Marine-Earth Science  
22 and Technology (JAMSTEC), 200 Monobe, Nankoku JAPAN, 783-8502.

23

24 \*Correspondence and requests for materials should be addressed to S.K.  
25 (kawagucci@jamstec.go.jp)

26

27

28

## **Supplementary information for Kawagucci et al.**

### **29 Contents of Supplementary Information**

- 30 1. Supplementary Methods
- 31 2. Supplementary Results
- 32 3. Supplementary Discussion
- 33 4. Supplementray Table
- 34 5. Supplementary Figures
- 35 6. References in this Supplementary Information

36

### **37 1. Supplementary Methods**

38 To know reference microbial cell densities in the deep-sea water of the Japan  
39 Trench regions, the deep-sea water (10 m above the seafloor) was sampled by the same  
40 method as in this study from 4 different stations from Stns. R, N1-N3 and JKEO (Stn. F:  
41 36°59.95'N-143°11.83'E at a water depth of 6800 m; Stn. 39N: 38°59.87'N-144°3.86'E  
42 at a depth of 6680 m; Stn. E: 38°15.27'N-144°2.24'E at a depth of 7415 m; Stn. SE:  
43 38°15.97'N-144°15.23'E at a depth of 6495 m) at a time of about 70 days after the 3.11  
44 Tohoku Earthquake during the JAMSTEC YK11-E03 R/V Yokosuka cruise.

45 For extraction of microbial DNA, quantitative PCR of 16S rRNA gene, and 16S  
46 rRNA gene clone analysis, a portion (2 L) of deep-sea water was filtered with a  
47 0.22- $\mu$ m-pore-size, 47-mm-diameter cellulose acetate filter (Advantec, Tokyo, Japan),  
48 was preserved onboard at -80 °C prior to DNA extraction. From the frozen filters with  
49 microbial communities, DNA was extracted by using the Ultra Clean Mega Soil DNA  
50 Isolation kit (MO Bio Laboratory, Solana Beach, CA, USA), following the  
51 manufacturer's instructions with minor modification. In the purification step, extracted  
52 DNA was concentrated by using spin filter unit provided in Ultra Clean Soil DNA  
53 Isolation kit (MO Bio Laboratory), and was eluted in 50 $\mu$ l. Quantitative PCR of  
54 archaeal and entire prokaryotic 16S rRNA genes was performed using 7500 Real Time  
55 PCR System following a method constructed by Takai & Horikoshi (2000) with minor  
56 modifications described previously (Nunoura et al., 2008). For amplification standards  
57 of archaeal and prokaryotic 16S rRNA genes, 16S rRNA gene mixtures described  
58 previously were used (Takai and Horikoshi, 2000).

59 Prokaryotic 16S rRNA gene clone analysis was conducted with another PCR  
60 experiment. Both bacterial and archaeal genes were simultaneously amplified from  
61 DNA extracts by PCR using LA Taq polymerase with GC buffer (TaKaRa Bio, Otsu,  
62 Japan). The oligonucleotide primers used were the mixtures of various derivatives of

63 previously designed 530F and 907R primers (Lane, 1985); the 530F primer mixture,  
64 (GTGCCAGCAGCCGCGG, GTGBCAGCCGCGCGG, YTGCCAGCCGCGCGG,  
65 GTGCCAGCAGCWGCGG, GTGCCAGCAGTCGCGG, GTGCCAGAAGMMTCGG  
66 and GTGGCAGTCGCCACGG), and 907R primer mixture  
67 (CCGYCAATTCMTTTRAGTTT, CCGYCTATTCCTTTGAGTTT,  
68 CCGYCAATTTCTTTRAGTTT, CCGYCAATTCCTTTRAGTTT,  
69 CCGYCAATTCCTTMAAGTTT and CCGCCAATTCCTTTGAATTT). Thermal  
70 cycling was performed under the following conditions: after initial preheating for 5 min  
71 at 96°C, denaturation at 96 °C for 25 sec, annealing at 50 °C for 45 sec, and extension at  
72 72 °C for 30 sec for a total of 35 cycles, and final extension at 72°C for 7 min. The PCR  
73 cycle numbers represent almost the minimum cycle numbers providing enough  
74 amplified products for the cloning based on the preliminary PCR amplification  
75 experiments using the same templates. The amplified rRNA gene products from several  
76 separate reactions at the least number of thermal cycles were pooled and purified as  
77 previously described (Takai et al., 2001). Cloning and sequencing were also followed  
78 by the procedure described by Takai et al. (2001). Approximately 450 nucleotides of  
79 cloned rRNA gene fragments were determined for single strand using M13M4  
80 oligonucleotide primer and the sequence similarity analysis was conducted among the  
81 clone sequences by using a similarity program in the GENETYX MAC software ver. 12  
82 (Genetyx Corporation, Tokyo, Japan). The sequences having >97% similarity were  
83 identified as the same phylotype. The sequences of the representative phylotypes were  
84 imported into the ARB software program (Ludwig et al., 2004) and were  
85 phylogenetically classified into certain taxonomic unit using Hugenholtz's small subunit  
86 rRNA sequence database and phylogenetic classification.

87 To assess difference in phylogenetic context of the post-earthquake deep-sea  
88 microbial communities in the bottommost deep-sea water, an online tool, UniFrac, was  
89 used for the principal coordinates analysis (PCoA). The UniFrac analysis was based on  
90 the phylogenetic tree that was reconstructed from the representative phylotypes in the  
91 clone libraries using the neighbor-joining method by ARB.

92

### 93 **3. Supplementary Results**

94 In the approx. 70-days-after deep-sea bottom water environments at 4 different  
95 stations from Stns. R, N1-N3 and JKEO, the increase of microbial cell densities in the  
96 bottom water samples was not obviously found. The average microbial cell density in  
97 the deep-sea water of the Japan Trench at 10 m above the seafloor at about 70 days after  
98 the largest earthquake (4 other stations) was determined to be  $1.1 \pm 0.12 \times 10^4$  cells ml<sup>-1</sup>

99 (Fig. 2). This average microbial cell density in the deep-sea water was used as a  
100 reference in an attempt to know the temporal and spatial variation of deep-sea microbial  
101 communities in biomass after the gigantic earthquake (Table S1).

102 The archaeal and prokaryotic 16S rRNA gene numbers in the whole microbial  
103 DNA assemblages were also determined (Table S1). The results showed quite similar  
104 patterns in spatial and temporal variation of microbial populations in the deep-sea  
105 bottom water environments as observed in the microbial cell densities (Fig. 2 and Table  
106 S1). In addition, the quantitative PCR showed that the archaeal rRNA gene proportions  
107 to the whole prokaryotic rRNA gene communities at the bottommost deep-sea water  
108 were 53.8, 33.7, 63.4, 63.5 and 89.7% at Stns. JKEO, R, N1, N2 and N3. These results  
109 suggested that all the deep-sea water microbial communities except for in the  
110 bottommost water at Stn. R could be dominated by the archaeal population.

111

### 112 **3. Supplementary Discussion**

113 The deep-sea temperature-salinity structures of our stations showed no spikes  
114 indicating inputs of hot fluid and/or freshwater (Fig. S2). Although local decrease of  
115 dissolved molecular oxygen (DO) in the depth profiles was found near the seafloor at  
116 Stns. N1 and N2, the parallel decrease in seawater density (Fig. S2) suggested that little  
117 in-situ DO consumption occurred through aerobic microbial activity, as observed in the  
118 Deepwater Horizon oil spill<sup>20</sup>. The depth of the slight pycnocline at Stn. N1 seems to be  
119 consistent with that of the methane and manganese peaks (Figs. 2 and S2). The  
120 disturbed vertical structure of seawater density would result from the usual internal  
121 wave induced by the interaction between tidal flow and topography (Vlasenko et al.,  
122 0225), although a tsunami-associated disturbance of the seawater structure cannot  
123 completely be ruled out as a possible alternative cause.

124 The 16S rRNA gene clone analysis of the bottommost deep-sea water revealed  
125 diverse but generally similar prokaryotic phylotype compositions among the stations  
126 (Fig. 3). The abundance of archaeal phylotypes in the whole microbial rRNA gene clone  
127 libraries was a little lower than that determined by the quantitative PCR analysis but  
128 supported the potential abundance of archaeal population in each of the deep-sea water  
129 microbial communities (Fig. 3). Commonly in all the bottommost deep-sea water  
130 samples, the phylotypes of *Gammaproteobacteria*, *Alphaproteobacteria*, *Bacteroidetes*,  
131 *Planctomycetes* and several subgroups of Marine Group I (MGI) archaea (or  
132 thaumararchaea) were identified as the predominant prokaryotic phylogenetic groups.  
133 There have been reported a few investigations of deep-sea planktonic prokaryotic  
134 phylotype compositions at depths of >1000 m (e.g., Lopez-Garcia et al., 2001) and no

135 previous example on the deep-sea planktonic microbial communities in the trench  
136 regions. Thus, it is difficult that the microbial phylotype compositions in the deep-sea  
137 water of the Japan Trench are compared to those in other geologically and  
138 geographically different deep-sea environments. Nevertheless, the similar predominant  
139 prokaryotic phylogenetic groups were also found in the deep-sea water samples (>2000  
140 m) in the North and mid Atlantic (Gallagher et al., 2004, Agogu e et al. 2011) and in  
141 the Antarctic (Lopez-Garcia et al., 2001). Thus, the planktonic microbial phylotype  
142 composition in the deep-sea water of the Japan Trench regions may represent the  
143 cosmopolitan nature.

144 In comparison of the bottommost water phylotype compositions among all the  
145 stations, some phylogenetic groups were detected in the deep-sea water samples at the  
146 trench landward slope stations. We tentatively defined signature phylogenetic groups in  
147 the post-earthquake deep-sea water as the phylogenetic groups that were identified in at  
148 least two stations of four trench landward slope stations and of which habitat endemism  
149 was obviously differentiated from the planktonic microbial communities in the ordinal,  
150 oxic deep-sea water habitats. For instances, SUP05 phylogroup within  
151 *Gammaproteobacteria* are the predominant planktonic microbial components with the  
152 possible sulfur-oxidizing chemolithoautotrophic potentials in the deep-sea hydrothermal  
153 fluid plumes (Sunamura et al., 2004) and in the oxygen minimum zones of ocean  
154 (Walsh et al., 2009), and may represent a fresh planktonic sulfur-oxidizing population  
155 that dominates the microbial communities in responding to the earthquake-induced  
156 sulfide input in the deep-sea water or to the sulfate reduction in colloidal sediment  
157 particle diffused by earthquake impact described below. Similarly, the  
158 zeta-proteobacterial phylotype was closely related with a deep-sea iron-oxidizing  
159 chemolithoautotroph, *Mariprofundus ferrooxydans* (Emerson et al., 2007), and with a  
160 number of rRNA gene phlotypes that dominated microbial communities in deep-sea  
161 iron-oxide mats of the hydrothermally active seafloors (Emerson et al., 2010). It is a  
162 possible inference that the zeta-proteobacterial phylotype in the bottommost deep-sea  
163 water is brought by the diffusing sediments with the existing seafloor microbial  
164 communities sustained by the ferrous iron-rich fluid seepages or is a newly dominating  
165 planktonic population sustained by chemical influx of ferrous iron to the deep-sea water  
166 via the earthquake-driven subseafloor fluid migration. Other potential signature  
167 phylogenetic phylogroups were *Desulfobacterales* and *Desulfuromonales* phylogroups  
168 within *Deltaproteobacteria* and *Arcobacter* phylogroup within *Epsilonproteobacteria*.  
169 The similar proteobacterial rRNA gene sequences have been found in the shallow  
170 sediments at and around the cold-seep chemosynthetic animal (*Calyptogenia* sp.)

171 colonies (Li et al., 1999; Inagaki et al., 2002). In addition, the phylogenetically related  
172 *Desulfobacterales*, *Desulfuromonales* and *Arcobacter* species are frequently identified  
173 as significant populations in the deep-sea benthic microbial communities of the anoxic  
174 and oxic-anoxic interface zones (Kuever et al., 2005a; 2005b; Vandamme et al., 2005;  
175 Wirsén et al., 2002). These proteobacterial phylotypes could be the existing benthic  
176 microbial components in the shallow sediments before the earthquakes and could be  
177 spread into the deep-sea water with the earthquake-induced sediment diffusion. In  
178 addition, the previously uncultivated euryarchaeota, DHVE5 and DHVE6, were initially  
179 found in the deep-sea hydrothermal vent chimneys and sediments hosting low  
180 temperatures of diffusing fluids (Takai and Horikoshi, 1999). However, several  
181 investigations clarified the occurrence of these previously uncultivated archaeal  
182 phylotypes in non-hydrothermal, but relatively reduced, marine sedimentary  
183 environments (Nakayama et al., 2011; Teske and Sørensen, 2008) although, intriguingly,  
184 typical seafloor archaeal phylogroups such as the DSAG (MBGB), SAGMEG and  
185 MCG (Teske and Sørensen, 2008) are absent in these deep waters. Thus, it seemed  
186 likely that these uncultivated archaeal phylogroups also represented the benthic  
187 microbial components spread into the deep-sea water by the earthquake-induced  
188 sediment diffusion, and grow in the colloidal microhabitats.

189         Probably the growths and functions of these signature microbial phylotypes  
190 and other phyloype components would be activated by the direct and indirect chemical  
191 inputs through the earthquake-induced sediment diffusion or seafloor fluid discharge.  
192 The increased microbial populations (microbial cell densities and prokaryotic 16S  
193 rRNA gene numbers) in the bottom water of the Japan Trench landward slope would  
194 represent such an activated response of the microbial community to the  
195 earthquake-induced environmental disturbances. In particular, the bottommost deep-sea  
196 water at Stn. R at the times of 36 and 98 days after the M9 event exclusively showed the  
197 increased abundance of bacterial 16S rRNA gene number in the whole prokaryotic 16S  
198 rRNA gene number (66.3 and 59.8 %, respectively) (Table S1). Since the 36-days-after  
199 bottommost deep-sea water at Stn. R had the highest LTA value (the greatest sediment  
200 diffusion), the potential enrichment of bacterial populations in the planktonic microbial  
201 communities is likely associated with the greatest influence of sediment diffusion. The  
202 certain chemical inputs in the deep-sea water such as the preserved seafloor reduced  
203 chemical substances (e.g., CH<sub>4</sub>, H<sub>2</sub>, sulfide, ferrous iron and organics) may trigger the  
204 selective activation that would more effectively work for the growths and functions of  
205 the bacterial components than the archaeal components in the planktonic microbial  
206 community.

207

208 **4. Supplementary Table**209 Table S1 Microbial cell density and archaeal and prokaryotic 16S rRNA gene number in  
210 whole microbial DNA assemblage in deep-sea bottom water environments

211

Station	Days after the M9 event	Altitude	Microbial cell density	Prokaryotic 16S rRNA gene number	Archaeal 16S rRNA gene number	Proportion of archaeal/prokaryotic 16S rRNA gene numbers
	(day)	(m)	(cells/ml)	(copy/ml)	(copy/ml)	(%)
JKEO	36	10	1.46 x 10 <sup>4</sup>	1.92 x 10 <sup>4</sup>	1.03 x 10 <sup>4</sup>	53.6
JKEO	36	381	1.56 x 10 <sup>4</sup>	1.32 x 10 <sup>4</sup>	0.94 x 10 <sup>4</sup>	71.2
JKEO	36	1381	2.01 x 10 <sup>4</sup>	1.77 x 10 <sup>4</sup>	0.83 x 10 <sup>4</sup>	46.9
R	36	10	3.01 x 10 <sup>4</sup>	8.58 x 10 <sup>4</sup>	2.89 x 10 <sup>4</sup>	33.7
R	98	10	0.83 x 10 <sup>4</sup>	0.87 x 10 <sup>4</sup>	0.35 x 10 <sup>4</sup>	40.2
R	36	110	3.32 x 10 <sup>4</sup>	n.d.*	n.d.	n.d.
R	36	310	1.62 x 10 <sup>4</sup>	n.d.	n.d.	n.d.
R	36	510	1.73 x 10 <sup>4</sup>	n.d.	n.d.	n.d.
R	36	760	1.96 x 10 <sup>4</sup>	3.47 x 10 <sup>4</sup>	1.69 x 10 <sup>4</sup>	48.2
R	98	760	0.99 x 10 <sup>4</sup>	0.78 x 10 <sup>4</sup>	0.37 x 10 <sup>4</sup>	48.1
R	36	1260	1.47 x 10 <sup>4</sup>	n.d.	n.d.	n.d.
N1	36	10	2.68 x 10 <sup>4</sup>	6.56 x 10 <sup>4</sup>	4.16 x 10 <sup>4</sup>	63.4
N1	36	160	1.71 x 10 <sup>4</sup>	n.d.	n.d.	n.d.
N1	36	280	1.60 x 10 <sup>4</sup>	n.d.	n.d.	n.d.
N1	36	400	1.77 x 10 <sup>4</sup>	n.d.	n.d.	n.d.
N1	36	550	2.12 x 10 <sup>4</sup>	3.60 x 10 <sup>4</sup>	2.37 x 10 <sup>4</sup>	65.8
N1	36	980	1.68 x 10 <sup>4</sup>	n.d.	n.d.	n.d.
N2	36	10	3.30 x 10 <sup>4</sup>	7.99 x 10 <sup>4</sup>	5.08 x 10 <sup>4</sup>	63.6
N2	98	10	1.90 x 10 <sup>4</sup>	1.72 x 10 <sup>4</sup>	0.92 x 10 <sup>4</sup>	53.5
N2	36	110	2.12 x 10 <sup>4</sup>	n.d.	n.d.	n.d.
N2	36	200	2.56 x 10 <sup>4</sup>	n.d.	n.d.	n.d.
N2	36	320	2.49 x 10 <sup>4</sup>	n.d.	n.d.	n.d.
N2	36	480	2.41 x 10 <sup>4</sup>	3.40 x 10 <sup>4</sup>	3.03 x 10 <sup>4</sup>	89.1
N3	36	10	2.04 x 10 <sup>4</sup>	5.08 x 10 <sup>4</sup>	4.56 x 10 <sup>4</sup>	89.8

N3	36	110	$2.93 \times 10^4$	n.d.	n.d.	n.d.
N3	36	950	$6.38 \times 10^4$	$10.2 \times 10^4$	$7.99 \times 10^4$	78.3
F	70	10	$1.22 \times 10^4$	n.d.	n.d.	n.d.
E	70	10	$1.11 \times 10^4$	n.d.	n.d.	n.d.
39N	70	10	$1.08 \times 10^4$	n.d.	n.d.	n.d.
SE	70	10	$0.93 \times 10^4$	n.d.	n.d.	n.d.

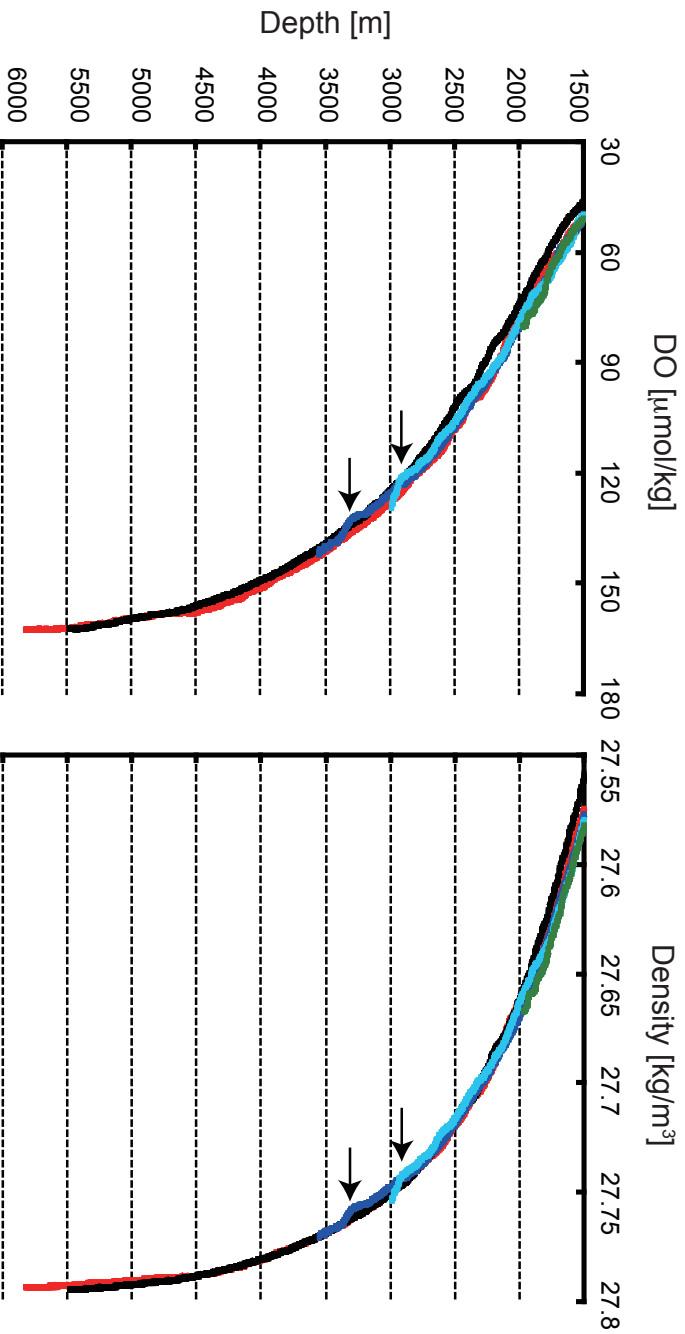
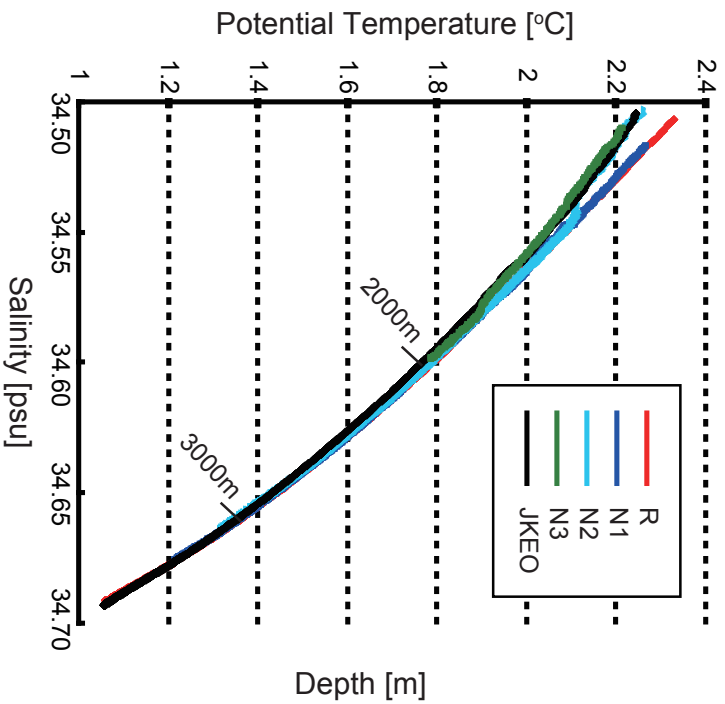
212 \*n.d.; not determined.

213

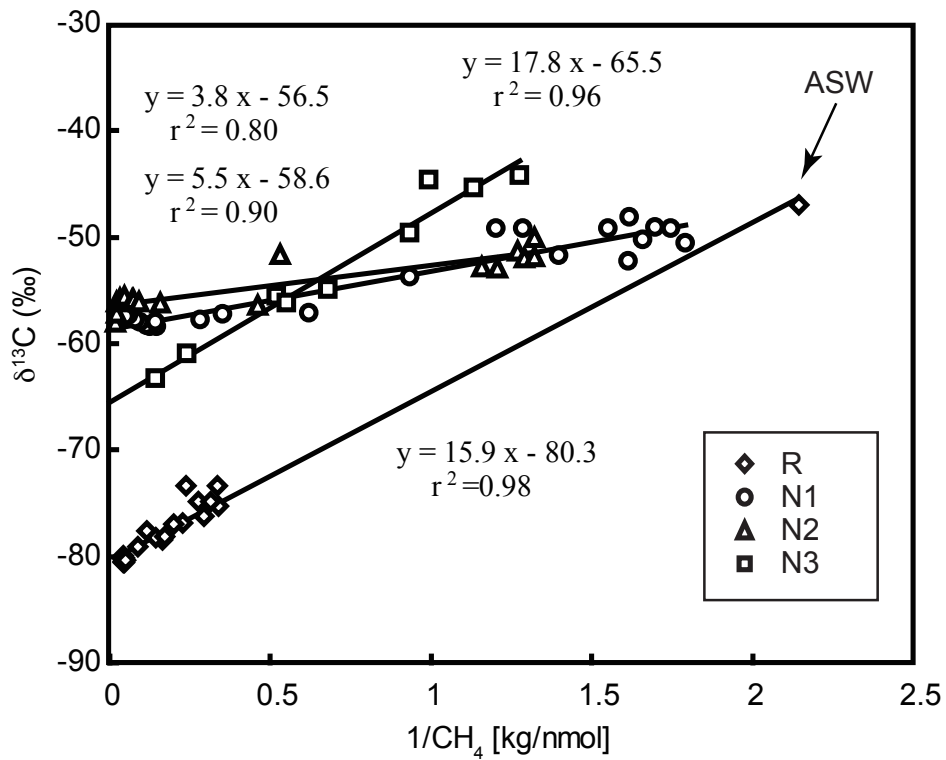
214 **5. Supplementary Figures**

215

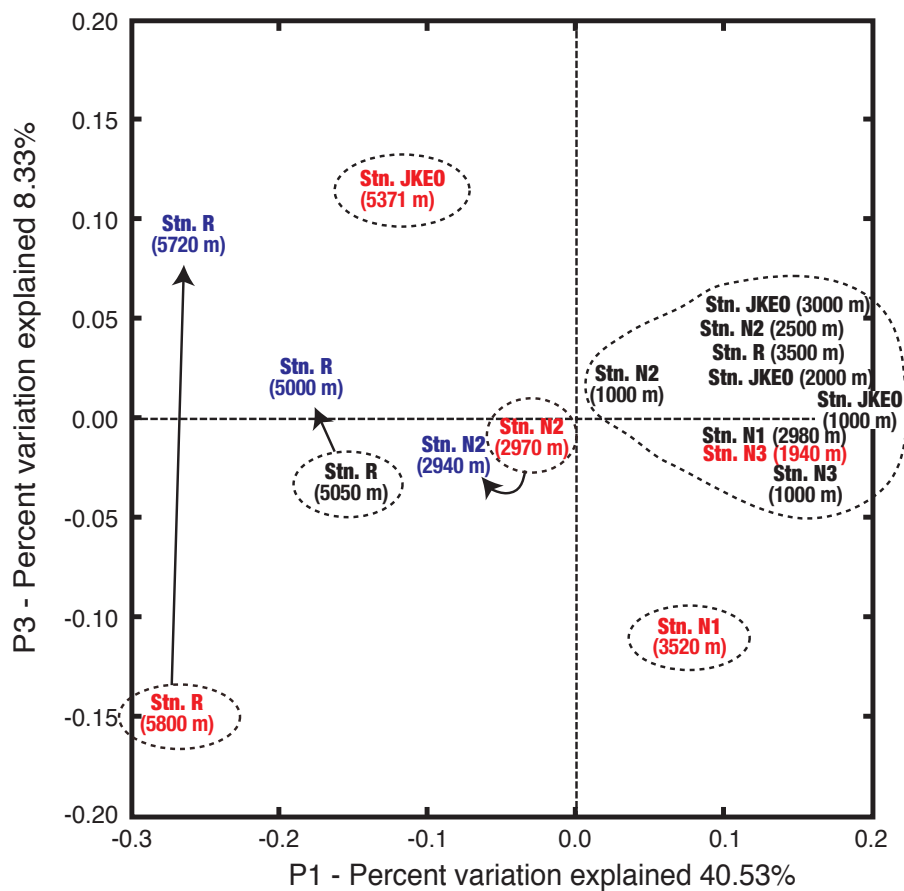




Supplementary Figure S1: Potential temperature, salinity, dissolved molecular oxygen and density in deep-sea water at the stations. The depths where decreases of dissolved molecular oxygen (DO) and density simultaneously occur at Stns. N1 and N2 are indicated by arrows.



Supplementary Figure S2: A Keeling plot of concentration and stable carbon isotopic composition of methane in deep-sea bottom water. A least-square line fitted to the data from each station is presented with the resulting equation and correlation coefficient.



Supplementary Figure S3: Comparison of post-earthquake prokaryotic phylotype compositions in the deep-sea bottom water environments of the Japan Trench region. The distribution pattern of the phylotype compositions at different stations was determined by the principal coordinates analysis using an online tool, UniFrac (Lozupone C et al., 2005). Red colors indicate the compositions in the 36-days-after deep-sea bottommost water at Stns. R, N1-3 and JKEO. Blue colors indicate the compositions in the 98-days-after deep-sea water at Stns. R and N2. Dot line areas show 6 types of brief classification of deep-sea water planktonic microbial phylotype compositions.

216 **6. References only in this Supplementary Information**

217 Inagaki, F. et al., *Environ Microbiol* **4**, 277 (2002).

218 Li, L. et al., *Mar Biotechnol* **1**, 391 (1999).

219 Nakayama, C. R. et al., *Deep-Sea Res Pt II* **58**, 128 (2011).

220 Nunoura, T. et al., *FEMS Microbiol Ecol* **64**, 240 (2008).

221 Takai, K., Horikoshi, K., *Appl Environ Microbiol* **66**, 5066 (2000).

222 Takai, K. et al., *Appl Environ Microbiol* **67**, 5750 (2001).

223 Teske, A, Sørensen, K. B., *ISME J* **2**, 3 (2008).

224 Vlasenko, V. et al., *Baroclinic Tides*, Cambridge University Press (2005).

225

226

227

228 Supplementary Figure S1: Potential temperature, salinity, dissolved molecular oxygen  
229 and density in deep-sea water at the stations. The depths where decreases of  
230 dissolved molecular oxygen (DO) and density simultaneously occur at Stns. N1 and  
231 N2 are indicated by arrows.

232 Supplementary Figure S2: A Keeling plot of concentration and stable carbon isotopic  
233 composition of methane in deep-sea bottom water. A least-square line fitted to the  
234 data from each station is presented with the resulting equation and correlation  
235 coefficient.

236 Supplementary Figure S3: Comparison of post-earthquake prokaryotic phylotype  
237 compositions in the deep-sea bottom water environments of the Japan Trench  
238 region. The distribution pattern of the phylotype compositions at different stations  
239 was determined by the principal coordinates analysis using an online tool, UniFrac  
240 (Lozupone C et al., 2005). Red colors indicate the compositions in the 36-days-after  
241 deep-sea bottommost water at Stns. R, N1-3 and JKEO. Blue colors indicate the  
242 compositions in the 98-days-after deep-sea water at Stns. R and N2. Dot line areas  
243 show 6 types of brief classification of deep-sea water planktonic microbial  
244 phylotype compositions.